Gasdermin E is required for induction of pyroptosis and severe disease during enterovirus 71 infection

Siwen Dong[1,2,‡], Yujin Shi[1,2,‡], Xiaojing Dong[1,2], Xia Xiao[1,2], Jianli Qi[1], Lili Ren[1,2], Zichun Xiang[1,2], Zhuo Zhou[3], Jianwei Wang[1,2,*], and Xiaobo Lei[1,2,*]

From the [1]NHC Key Laboratory of Systems Biology of Pathogens, Institute of Pathogen Biology, and [2]Key Laboratory of Respiratory Disease Pathogenomics, Chinese Academy of Medical Sciences and Peking Union Medical College, Beijing, P.R. China; [3]Biomedical Pioneering Innovation Center, Beijing Advanced Innovation Center for Genomics, Peking University Genome Editing Research Center, School of Life Sciences, Peking University, Beijing, China

Edited by Peter Cresswell

Pyroptosis is an inflammatory form of programmed cell death that is executed by the gasdermin (GSDM)-N domain of GSDM family proteins, which form pores in the plasma membrane. Although pyroptosis acts as a host defense against invasive pathogen infection, its role in the pathogenesis of enterovirus 71 (EV71) infection is unclear. In the current study, we found that EV71 infection induces cleavage of GSDM E (GSDME) by using western blotting analysis, an essential step in the switch from caspase-3-mediated apoptosis to pyroptosis. We show that this cleavage is independent of the 3C and 2A proteases of EV71. However, caspase-3 activation is essential for this cleavage, as GSDME could not be cleaved in caspase-3-KO cells upon EV71 infection. Further analyses showed that EV71 infection induced pyroptosis in WT cells but not in caspase-3/GSDME double-KO cells. Importantly, GSDME is required to induce severe disease during EV71 infection, as GSDME deficiency in mice was shown to alleviate pathological symptoms. In conclusion, our results reveal that GSDME is important for the pathogenesis of EV71 *via* mediating initiation of pyroptosis.

Hand, foot, and mouth disease (HFMD) caused by enterovirus A species infection is an infectious disease in young children, particularly those under 5 years of age in the Asia–Pacific region, since it was first confirmed in California in 1974 (1–6). Most infections are self-limiting, usually with fever, mouth sores, and vesicular rash on the hands, feet, and mouth. However, some can cause severe neurological diseases in children, which include aseptic meningitis, acute flaccid paralysis, encephalitis, and pulmonary edema (7–10). Almost all these severe complications are caused by enterovirus 71 (EV71) in young children and infants. Similarly, EV71-infected mice less than 5 days of age are typically symptomatic (11–13). While host immunity may be involved, the precise mechanism remains largely unclear.

Pyroptosis is caspase-1-mediated cell death, characterized by cellular swelling and membrane blebbing (14, 15). During the process of pyroptosis, the cell membrane becomes porous and intracellular substances are released into the supernatant, which induce a proinflammatory response (16). Recent evidence has shown that pyroptosis relies on gasdermin (GSDM) family protein, encoded by GSDM-related genes that include GSMDA, GSDMB, GADMC, GSDMD, GEDME (DFNA5), and DFNB59 (17–19). Shi *et al.* (17) found that GSDMD is a substrate of caspase-1 and caspase-4/5/11 that mediate pyroptosis and interleukin (IL)-1β secretion. Upon inflammasome activation, GSDMD is cleaved into GSDMD-N and GSDMD-C fragments (20–23). Consequently, the cleaved N-terminal fragment of GSDMD triggers pyroptosis by binding to membrane lipids and forming pores in the cytoplasmic membrane (17–23).

GSDME, another member of the GSDM family, also possesses the functional N-terminal domain that induces pyroptosis (24). However, it is not susceptible to inflammatory caspases, such as caspase-1, caspase-4, caspase-5, or caspase-11, in mammalian cells (24). Recently, Wang *et al.* (24) reported that GSDME is a substrate of caspase-3. Upon cleavage, it produces a GSDME-N fragment that switches chemotherapeutic drug–induced apoptosis to pyroptosis (24). Similar data have obtained in macrophages treated with etoposide or infected with vesicular stomatitis (25). GSDME also permeabilizes the mitochondrion membrane, induces cytochrome *c* release, and activates the apoptosome (26). However, the role of GSDME in enterovirus-induced cell death is unknown.

Here, we report that EV71 infection induces pyroptosis through GSDME. Specifically, EV71 infection activates caspase-3, which cleaves GSDME at the amino acid pair of D270–E271. Remarkably, GSDME-deficient mice exhibit delayed onset of neurological symptoms and survive longer than WT mice upon EV71 infection. These results revealed that GSDME plays a critical role in the pathogenesis of EV71.

Results

EV71 induces cell pyroptosis

To better understand pyroptosis during EV71 infection, we established an EV71 infection model to measure lactate dehydrogenase (LDH) release and ATP production. As shown in Figure 1A, EV71 infection resulted in a significant increase

‡ These authors contributed equally to this work.
* For Correspondence: Xiaobo Lei, fyleixb@126.com; Jianwei Wang, wangjw28@163.com.

of LDH release in a dose-dependent manner compared with mock-infected cells, which indicated that EV71 infection disrupted cell membrane integrity. Similar results were observed in cell viability analyses (Fig. 1*B*). Immunofluorescence staining revealed active EV71 replication in HeLa cells (Fig. 1*C*). Cell morphological analysis showed that EV71 infection induced cell death with characteristics of cell swelling and large bubbles from the plasma membrane after infection (Fig. 1*D*). Taken together, these data indicated that EV71 infection induced cell death, possibly by pyroptosis.

EV71 infection induces cleavage of GSDME independently of 3C and 2A proteases

To assess whether GSDME is critical for EV71-induced pyroptosis, we examined the expression level of GSDME after EV71 infection. HeLa and SK-N-SH cells were mock infected or infected with EV71. At various time points after infection, cell lysates were prepared for Western blot (WB)

analysis. Figure 2 shows that GSDME was expressed in mock-infected HeLa (Fig. 2*A*) and SK-N-SH (Fig. 2*B*) cells. EV71 infection induced cleavage of GSDME in these cells (Fig. 2, *A* and *B*) in a time-dependent manner. Further analysis showed that EV71 acted in a dose-dependent manner (Fig. 2, *C* and *D*). Indeed, EV71 replicated in these cell lines as measured by VP0 and VP2 (Fig. 2, *A–D*). These phenotypes were recapitulated in rhabdomyosarcoma (RD) and 293T cells. A similar phenotype was observed in RD and 293T cells (Fig. 2, *E* and *F*). These results indicated that EV71 infection induces cleavage of GSDME in host cells, which suggests that GSMDE is a critical factor for EV71-induced pyroptosis.

To investigate the molecular mechanisms, we constructed a plasmid to express GSDME with Myc and FLAG tag in the N terminus and C terminus, respectively. After plasmid transfection, 293T cells were mock infected or infected with increasing doses of EV71. At 24 h postinfection, cell lysates were prepared to examine EV71-mediated cleavage of GSDME
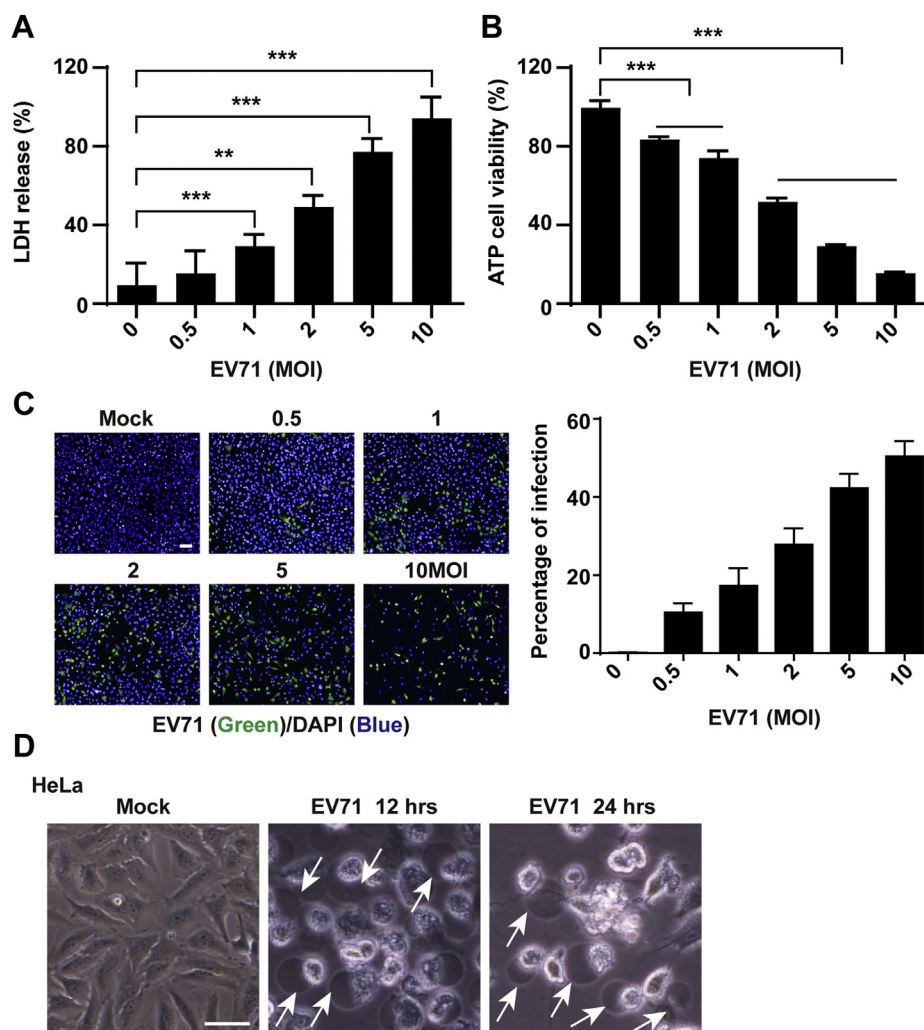

Figure 1. EV71 infection induces pyroptosis. *A* and *B*, HeLa cells were mock infected or infected with EV71 at various MOIs as indicated. At 24 h after infection, LDH release–based cell death (*A*) and ATP cell viability were assessed. *C*, EV71 replication in HeLa cells. After infection, HeLa cells were fixed and stained with an antibody against EV71 (*green*). Nuclei were counterstained with DAPI (*blue*). The scale bar represents 100 μm. *D*, pyroptosis induced by EV71 infection. HeLa cells were mock infected or infected with EV71. At the indicated time points, phase-contrast imaging was performed. Images were obtained by microscopy. The scale bar represents 50 μm. All data are mean values ± SD. Experiments were performed as triplicates and repeated at least twice. *$p < 0.05$, **$p < 0.01$, and ***$p < 0.001$. DAPI, 4′,6-diamidino-2-phenylindole; EV71, enterovirus 71; LDH, lactate dehydrogenase; MOI, multiplicity of infection.
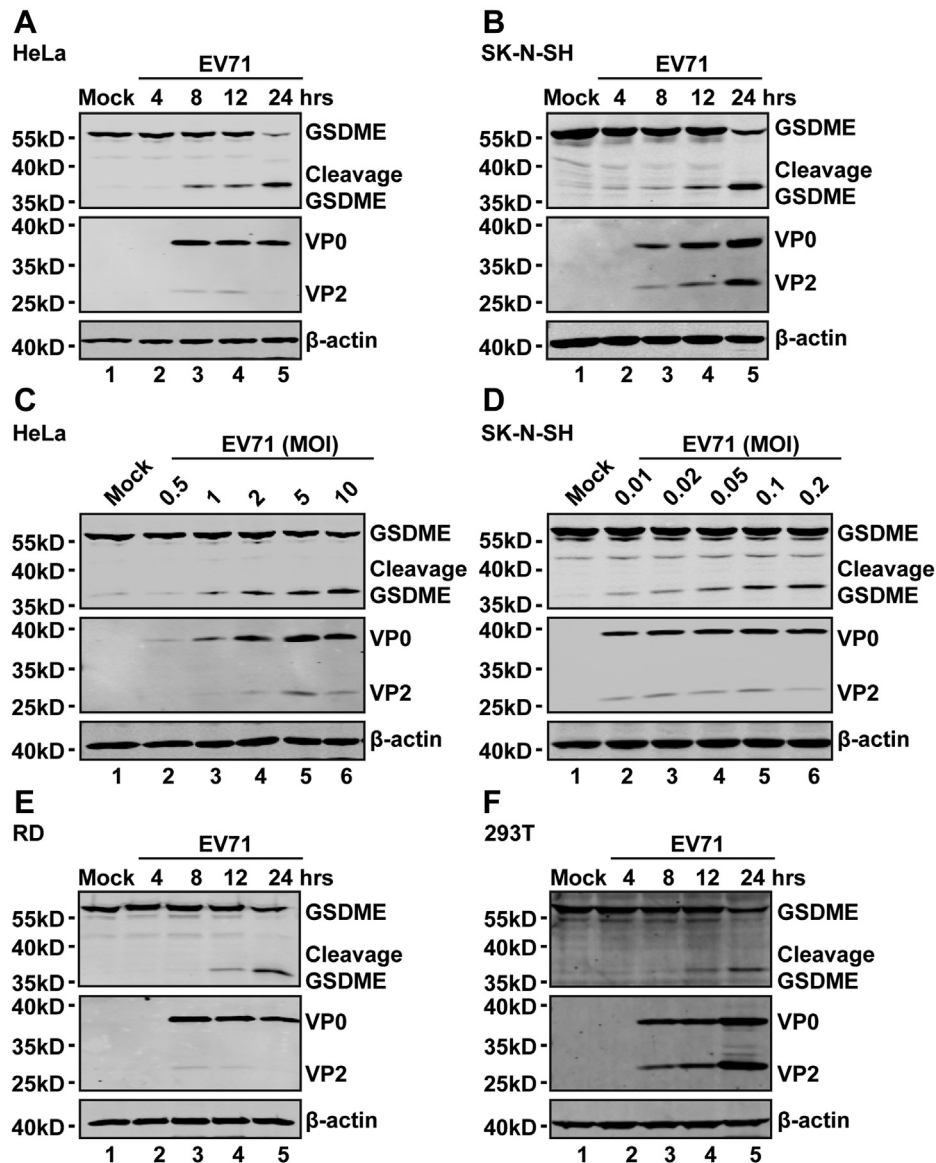
Figure 2. EV71 infection induces the cleavage of GSDME. *A* and *B*, HeLa (*A*) and SK-N-SH (*B*) cells were mock infected or infected with EV71 at MOIs of 2 or 0.2, respectively. At the indicated time points, cell lysates were analyzed by Western blotting with antibodies against GSDME, which recognized the N-terminal region of GSDME, EV71, and β-actin. *C* and *D*, HeLa (*C*) and SK-N-SH (*D*) cells were infected with EV71 at various MOIs as indicated for 24 h. Cell lysates were analyzed by Western blotting as described in (*A*) and (*B*). *E* and *F*, RD (*E*) and 293T (*F*) cells were mock infected or infected with EV71. At the indicated time points, cell lysates were analyzed as described in (*A*) and (*B*). Data are representative of three independent experiments. EV71, enterovirus 71; GSDME, gasdermin E; MOI, multiplicity of infection; RD, rhabdomyosarcoma.

by WB. We found two small protein bands when cells were infected with EV71. These small bands were the N-terminal fragment (approximately 30 kDa) and C-terminal fragment (approximately 20 kDa), respectively. Therefore, EV71 infection induced cleavage of overexpressed GSDME in a dose-dependent fashion in 293T cells (Fig. 3A). In addition, only one band was detectable by each antibody, which indicated that EV71 induced GSDME cleavage at a single site. To explore whether GSDME is a target of EV71 3C and 2A, we conducted a cleavage assay. As shown in Figure 3, *B* and *D*, ectopic expression of 3C or 2A in 293T cells had no effect on the cleavage of GSDME. However, interferon regulatory factor 7 was cleaved by EV71 3C protease (Fig. 3C), which was used as a positive control. Similarly, eukaryotic translation initiation

factor 4G was used as a positive control for 2A cleavage (Fig. 3D). These results suggest that EV71 infection induces GSDME cleavage at only one site, which is independent of EV71 2A and 3C proteases.

EV71-induced cleavage of GSDME is dependent on activation of caspase-3

It has been reported that caspase-3 cleaves GSDME after tumor necrosis factor alpha or etoposide stimulation (24, 25). To examine the effect of EV71, we analyzed GSDME in virus-infected cells. As shown in Figure 3A, EV71 infection resulted in a cleavage pattern similar to that mediated by etoposide, which suggested that EV71-induced cleavage of GSDME may involve caspase-3. To test this hypothesis, we first determined
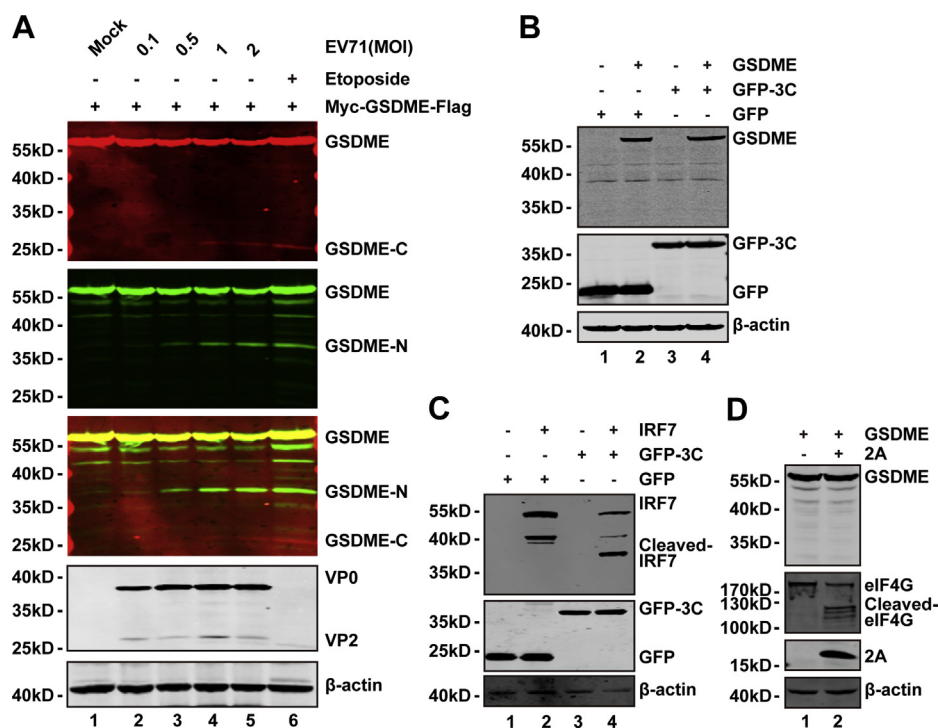
Figure 3. EV71-mediated cleavage of GSDME is independent on 2A and 3C proteases. *A*, 293T cells were transfected with a plasmid that encoded Myc-GSDME-FLAG (lanes 1–6). At 24 h after transfection, the cells were mocked infected or infected with increasing doses of EV71. At 24 h after infection, cell lysates were analyzed by Western blotting with the indicated antibodies using the LI-COR Odyssey Dual-Color System (LI-COR). Antibodies that recognized Myc-GSDME-FLAG (Myc, N-terminal region of GSDME, 800 nm, *green*; FLAG, C-terminal region of GSDME, 680 nm, *red*) were used. The merged images of the two channels are shown below (*yellow*). EV71 was detected by using an antibody that recognized VP0 and VP2. β-actin was detected as a loading control. Etoposide was used as a control. *B*, 293T cells were transfected with plasmids that encoded GSDME (lanes 2 and 4) and GFP (lanes 1 and 2) or GFP-3C (lanes 3 and 4). At 24 h after transfection, the cells were prepared for Western blotting analyses using antibodies against Myc, GFP, and β-actin. *C*, 293T cells were transfected with plasmids that encoded IRF7 (lanes 2 and 4) along with GFP (lanes 1 and 2) or GFP-3C (lanes 3 and 4). Cells were analyzed as described in (*B*). *D*, 293T cells were transfected with a plasmid that encoded GSDME along with a control plasmid or pcDNA3.1-IRES-2A plasmid. At 24 h after transfection, cells were lysed and analyzed by Western blotting using antibodies against Myc, V5, and eIF4G. Data are representative of three independent experiments. eIF4G, eukaryotic translation initiation factor 4G; EV71, enterovirus 71; GSDME, gasdermin E; IRF7, interferon regulatory factor 7.

whether EV71 infection induces caspase-3 activation. As illustrated in Figure 4, EV71 infection induced processing of caspase-3 in HeLa (Fig. 4A) and SK-N-SH (Fig. 4B) cells in a dose-dependent manner. Furthermore, caspase-3 was activated in a time-dependent manner upon EV71 infection (Fig. 4, *C* and *D*).

Previous studies have demonstrated that human GSDME has a caspase-3-cleavable site, namely 267DMPD270 (24, 25). To investigate whether EV71-mediated GSDME cleavage occurs at this site, we conducted a cleavage experiment using the D270A mutant (Fig. 5A). The 293T cells were transfected with plasmids that expressed WT GSDME or D270A mutant GSDME. At 24 h after transfection, the cells were mock infected or infected with EV71 with an increased multiplicity of infection. After 24 h, cell lysates were prepared to examine EV71-mediated cleavage of GSDME or its derivative with the D270A substitution by WB. As shown in Figure 5B, EV71 infection resulted in cleavage of WT GSDME but not the D270A mutant. These results show that D270 is a critical site for EV71-induced GSDME cleavage.

To evaluate whether caspase-3 is necessary for GSDME cleavage, we generated a caspase-3$^{-/-}$ cell line by CRISPR–CRISPR-associated protein 9 technology (Fig. 5C). As expected, in caspase-3-KO cells, caspase-3 expression was

absent (Fig. 5C, *lower*). Upon infection of the caspase-3$^{-/-}$ cells with EV71, GSDME remained intact (Fig. 5D, *right*) compared with WT cells (Fig. 5D, *left*). To limit the possibility of off-target activities of the CRISPR construct, we established new single-cell clones for caspase-3 KO. Then, two single-cell clones were mock infected or infected with EV71. Upon infection, a similar phenotype of GSDME cleavage was found (Fig. 5E). For confirmation, we rescued caspase-3 in KO cell lines. When expressed ectopically, caspase-3 restored GSDME cleavage in caspase-KO cell lines (Fig. 5F). These data suggest that caspase-3 is necessary for EV71-mediated cleavage of GSDME.

Caspase-3 and GSDME are necessary for EV71-induced pyroptosis

The aforementioned results show that EV71 induces caspase-3-dependent GSDME cleavage and pyroptosis. Next, we examined whether EV71-induced pyroptosis is directly related to GSDME and caspase-3. First, we established a *Gsdme*$^{-/-}$ cell line by CRISPR–CRISPR-associated protein 9 technology (Fig. 6A, *left*), in which GSDME expression was eliminated (Fig. 6A, *right*). Next, we established a double GSDME$^{-/-}$ and caspase-3$^{-/-}$ cell line (Fig. 6B, *left*). These cell lines were verified by DNA sequencing and WB analysis (Fig. 6B), which
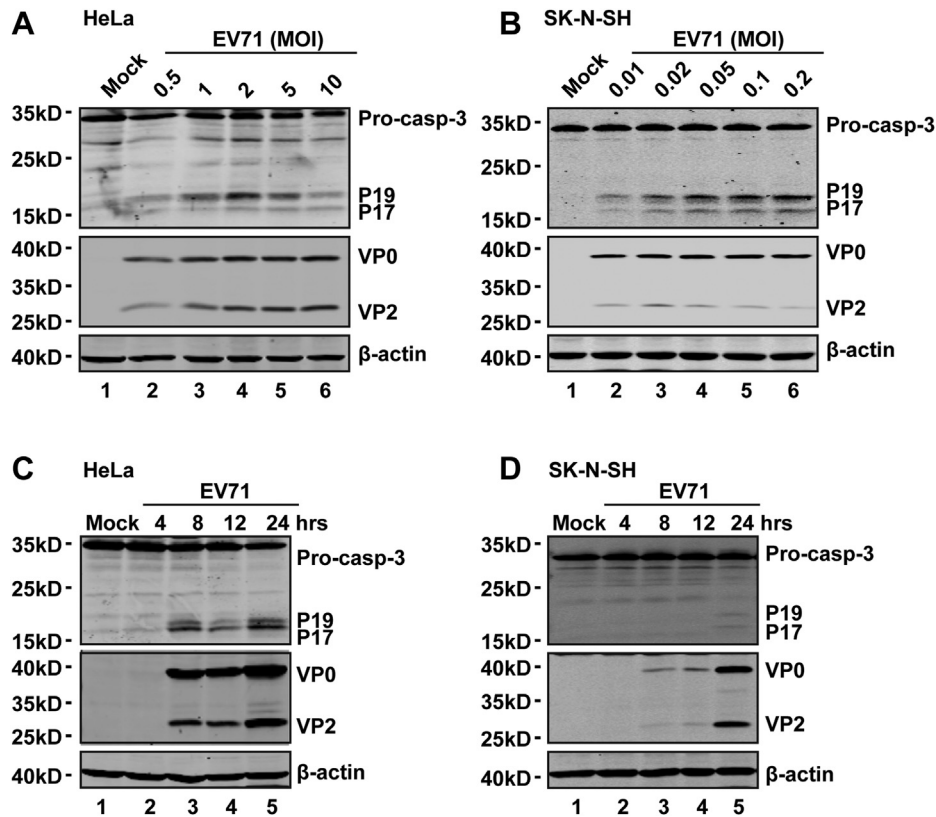
Figure 4. EV71 induces activation of caspase-3. *A* and *B*, HeLa (*A*) and SK-N-SH (*B*) cells were infected with EV71 at various MOIs as indicated for 24 h. Cell lysates were analyzed by Western blotting. *C* and *D*, HeLa (*C*) and SK-N-SH (*D*) cells were mock infected or infected with EV71 at MOIs of 2 or 0.2, respectively. At the indicated time points, cell lysates were analyzed by Western blotting with antibodies against caspase-3, EV71, and β-actin. Data are representative of three independent experiments. EV71, enterovirus 71; MOI, multiplicity of infection.

showed no expression of caspase-3 and GSDME in double-KO cells. Furthermore, we assessed the EV71-induced cell death in these cells. LDH release and ATP cell viability assays showed that the LDH release was reduced in caspase-3 or GSDME-KO cells, particularly in double-KO cells compared with WT cells (Fig. 6, *C* and *D*). Phase-contrast images showed that EV71 induced pyroptosis in WT cells but not in double-KO cells (Fig. 6E). In caspase-3$^{-/-}$ or GSDME$^{-/-}$-KO cells, EV71 infection induced cell death, but cell swelling was not observed (Fig. 6E). Thus, caspase-3 and GSDME are necessary for EV71-induced pyroptosis. Compared with WT cells, the viral proteins were almost identical in caspase 3$^{-/-}$ and *Gsdme*$^{-/-}$ cell lines. However, the viral proteins were slightly decreased in double-KO cells (Fig. 6F), which indicated that disruption of apoptosis and pyroptosis in double-KO cells might inhibit virus release. Taken together, these data illustrate that GSDME switched EV71-induced apoptosis to pyroptosis in GSDME-expressing cells.

GSDME deficiency delays the onset of neurological symptoms upon EV71 infection

The role of GSDME in the pathogenesis of EV71 was further investigated *in vivo*, using the model of EV71 infection as described previously (27). Suckling mice were infected with EV71 virus through intraperitoneal injection. Subsequently, growth slowed down at 4 days postinfection (DPI) in WT mice

but not in *Gsdme*$^{-/-}$ mice (Fig. 7A). Most mice had clinical symptoms at 4 DPI (data not shown). As shown in Figure 7B, WT mice displayed significantly higher mortality compared with *Gsdme*$^{-/-}$ mice, which indicated that GSDME facilitates EV71 pathogenesis *in vivo*. Congruently, EV71-infected *Gsdme*$^{-/-}$ mice survived longer than EV71-infected WT mice. Next, we assessed the production of proinflammatory cytokines associated with HFMD. The cytokines in peripheral blood from WT and *Gsdme*$^{-/-}$ mice infected with EV71 were measured at 3 DPI. The results showed that expression of IL-6 and monocyte chemoattractant protein-1 was decreased in *Gsdme*$^{-/-}$ mice (Fig. 7, *D* and *E*), but the expression level of tumor necrosis factor alpha was unchanged (Fig. 7C). Comparable levels of EV71 mRNA were detected in muscles, intestines, and brains of *Gsdme*$^{-/-}$ and WT mice, which suggested that GSDME did not affect viral replication (Fig. 7, *F–H*). These results suggest that GSDME-dependent pyroptosis is linked to inflammation, which may contribute to EV71 pathogenesis.

Discussion

EV71 is a causative agent of HFMD in children younger than 5 years of age. In addition, some patients show severe neurological diseases (2–7). Accumulating evidence suggests that virus-induced cell death and proinflammatory cytokines are important components of host defense against EV71 infection
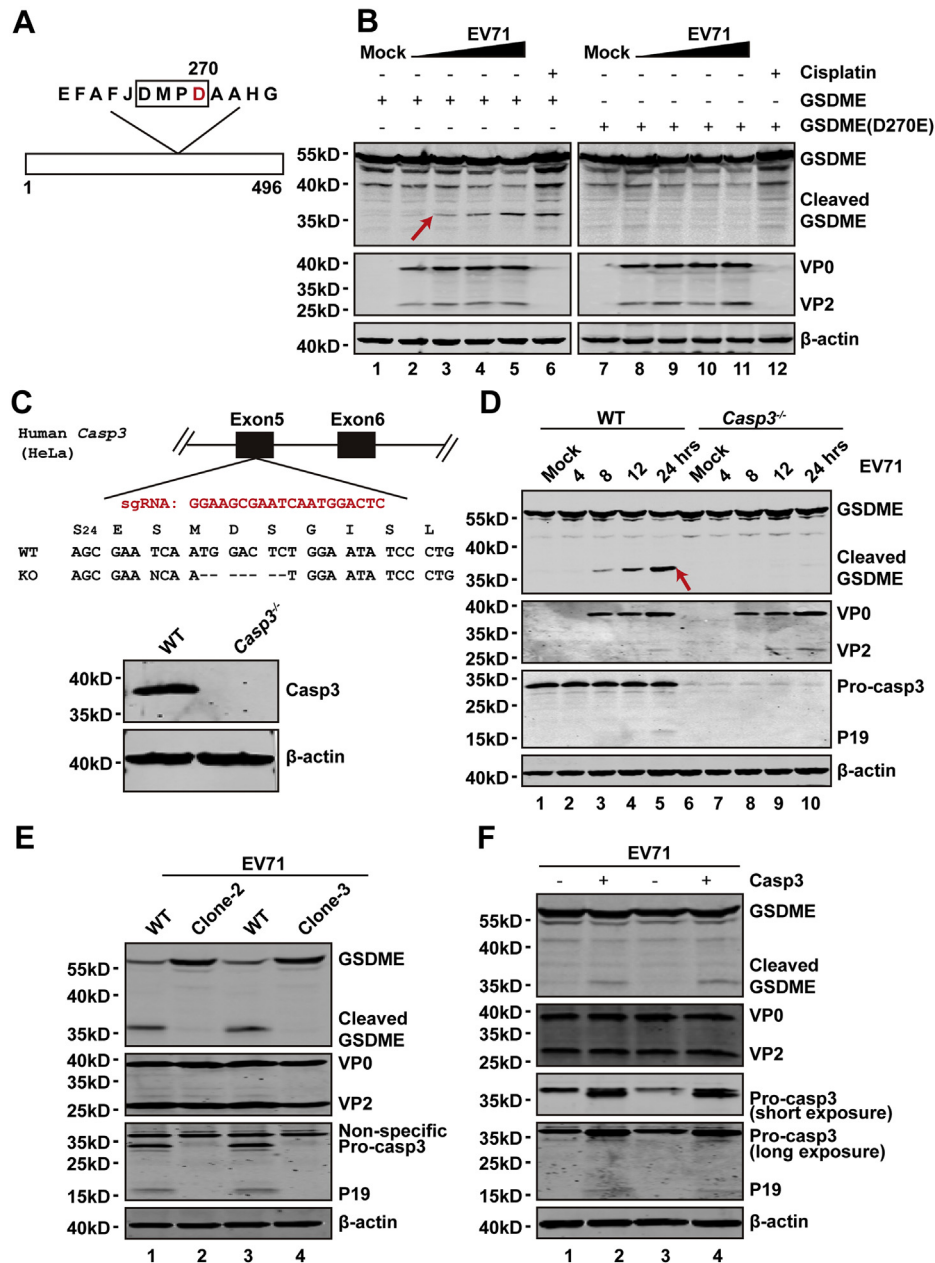
SASBMB

J. Biol. Chem. (2022) 298(5) 101850 **5**

Figure 5. EV71-mediated cleavage of GSDME is dependent on activation of caspase-3. *A*, primary sequences of amino acids 262 to 274 in GSDME. *B*, 293T cells were transfected with plasmids that encoded WT GSDME or D270A mutant GSDME. At 24 h after transfection, cells were mock infected or infected with EV71 at increasing doses for 24 h. Cell lysates were analyzed by Western blotting. *C*, Casp3⁻/⁻ HeLa cells were generated by CRISPR–CRISPR-associated protein 9 (Cas9)–mediated genome editing. The upper of (*C*) shows a related portion of the caspase-3 genomic structure. The single-guide RNA sequence is shown in *red*, which resided in exon 5 of caspase-3. Sequences of the targeted region and KO are shown. The lower of (*C*) shows expression of caspase-3 in WT and KO cells. *D*, WT and caspase-3-KO cells were infected with EV71. At the indicated times, cells were collected and lysates were analyzed by Western blotting. Data are representative of three independent experiments. *E*, the WT HeLa and other clones of Casp3⁻/⁻ HeLa cells were infected with EV71. At 24 h, cells were collected and lysates were analyzed by Western blotting. *F*, the plasmid that expresses caspase-3 was transfected into the Casp3⁻/⁻ HeLa cells. After 24 h, cells were infected with EV71. At 24 h, the GSDME cleavage and caspase-3 expression were detected by Western blotting. EV71, enterovirus 71; GSDME, gasdermin E.

(7, 28–33). Pyroptosis and necroptosis are two forms of programmed cell death, which are associated with the production of proinflammatory cytokines (22, 34–37). However, their roles remain to be defined in EV71 infection. Bai *et al.* (38) showed that EV71 infection mainly induces apoptosis with characteristic cell shrinkage, nuclear condensation, and a decreased mitochondrial potential. Neither GSDMD-mediated pyroptosis nor phosphorylatedMLKL–mediated necroptosis

was seen. However, Wang *et al.* and our previous studies (33, 39, 40) suggest that EV71 infection activates NLRP3 (NOD-, LRR-, and pyrin domain–containing protein 3)–inflammasome formation and induces the secretion of IL-1β and IL-18, which indicates that EV71 infection induces pyroptosis, but GSDMD cleavage by caspase-1 was not assessed in these studies. Our results showed that the 3C protease cleaves GSDMD at the Q193–G194 pair, which results in a truncated N-terminal
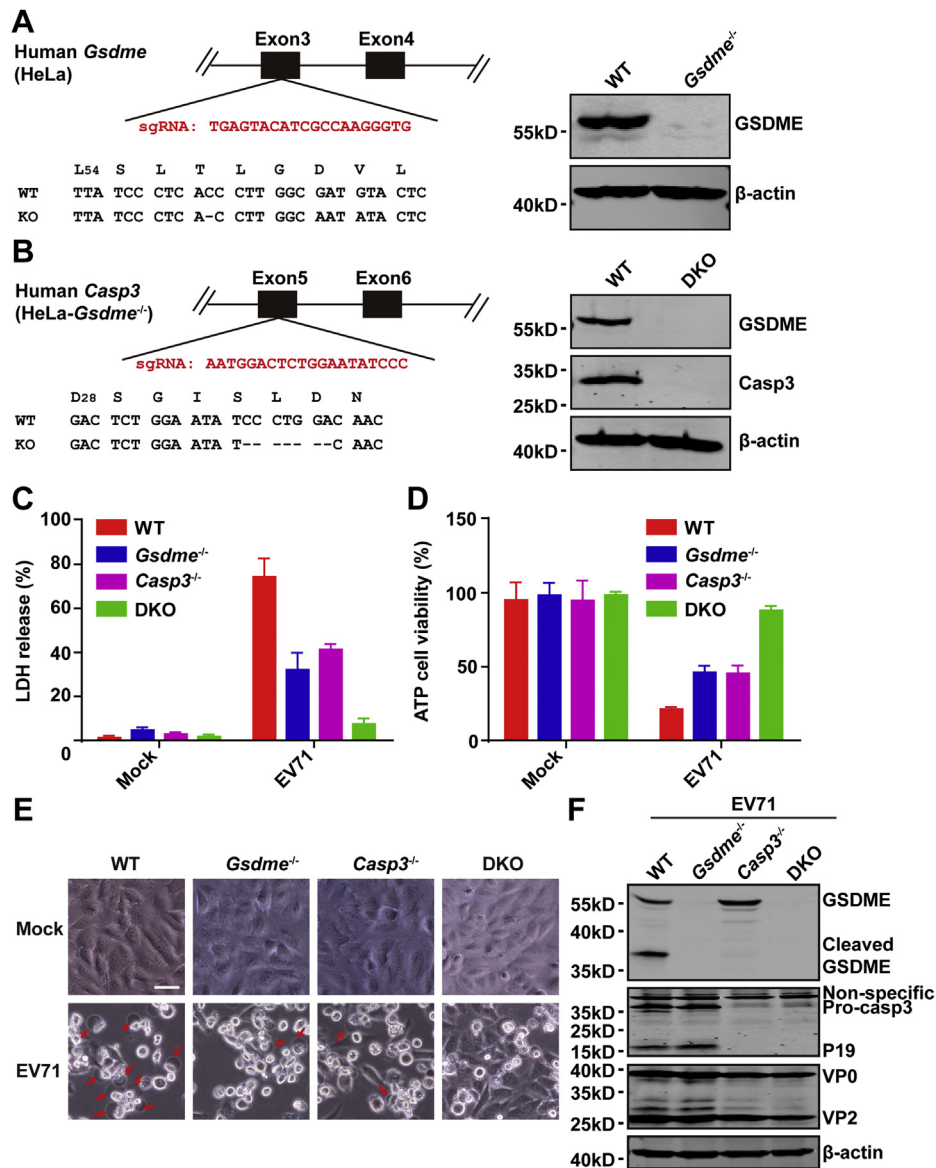
Figure 6. GSDME and caspase-3 are necessary for EV71-mediated pyroptosis. *A*, generation of *Gsdme*$^{-/-}$ HeLa cells by CRISPR–CRISPR-associated protein 9 (Cas9)–mediated genome editing. The *right panel* shows a related portion of the GSDME genomic structure. The single-guide RNA (sgRNA) sequence is shown in *red*. One screen-positive clone of *Gsdme*$^{-/-}$ was detected by Western blotting. *B*, generation of caspase-3 and GSDME double-KO (DKO) HeLa cells. DKO cells were established using as sgRNA of caspase on the basis of *Gsdme*$^{-/-}$ HeLa cells. The sgRNA sequence of caspase-3 is shown in *red*. Expression of caspase-3 and GSDME was detected in the DKO cells by Western blotting. *C* and *D*, *Gsdme*$^{-/-}$, *caspase 3*$^{-/-}$, and DKO cells were mock infected or infected with EV71 at an MOI of 2. At 24 h after infection, LDH release–based cell death (*C*) and ATP cell viability (*D*) were detected. *E* and *F*, EV71-induced pyroptosis and viral replication in WT, *caspase 3*$^{-/-}$, *Gsdme*$^{-/-}$, and DKO cells. The four cell lines were infected with EV71 at an MOI of 2. After 24 h, phase-contrast imaging was performed. Images were obtained by microscopy. The scale bar represents 50 μm. Cell lysates were prepared for Western blotting. All data are mean values ± SD. Experiments were performed as triplicates and repeated at least twice. *$p < 0.05$, **$p < 0.01$, and ***$p < 0.001$. Data are representative of three independent experiments. EV71, enterovirus 71; GSDME, gasdermin E; MOI, multiplicity of infection.

fragment to perturb pyroptosis mediated by the 1-275 N-terminal fragment of GSDMD (40). Our study suggests that GSDME-mediated pyroptosis is critical to determine the pathogenesis of EV71.

We used an LDH release assay and morphological observation to evaluate cell death induced by EV71 infection in HeLa and SK-N-SH cells. The LDH release assay and morphological change are useful tools to detect pyroptosis (17). EV71 infection induces release of LDH and typical pyroptotic morphology, which indicates that EV71 infection induces pyroptosis in HeLa and SK-N-SH cells (Fig. 1).

Recently, it has been reported that GSDME switches chemotherapeutic drug–induced apoptosis to pyroptosis in a caspase-3-dependent manner (24, 25). However, the precise role of GSDME in enterovirus-induced cell death remained elusive. We found that EV71 infection induces cleavage of GSDME in dose-dependent and time-dependent manners (Fig. 2), suggesting that GSDME is important for EV71-mediated cell death.

Upon activation of caspases, GSDMD is cleaved by caspase-1 at the D275-G276 pair, which releases its N-terminal domain GSDMD$_{1-275}$ (17). However, EV71 3C cleaves GSDMD at the
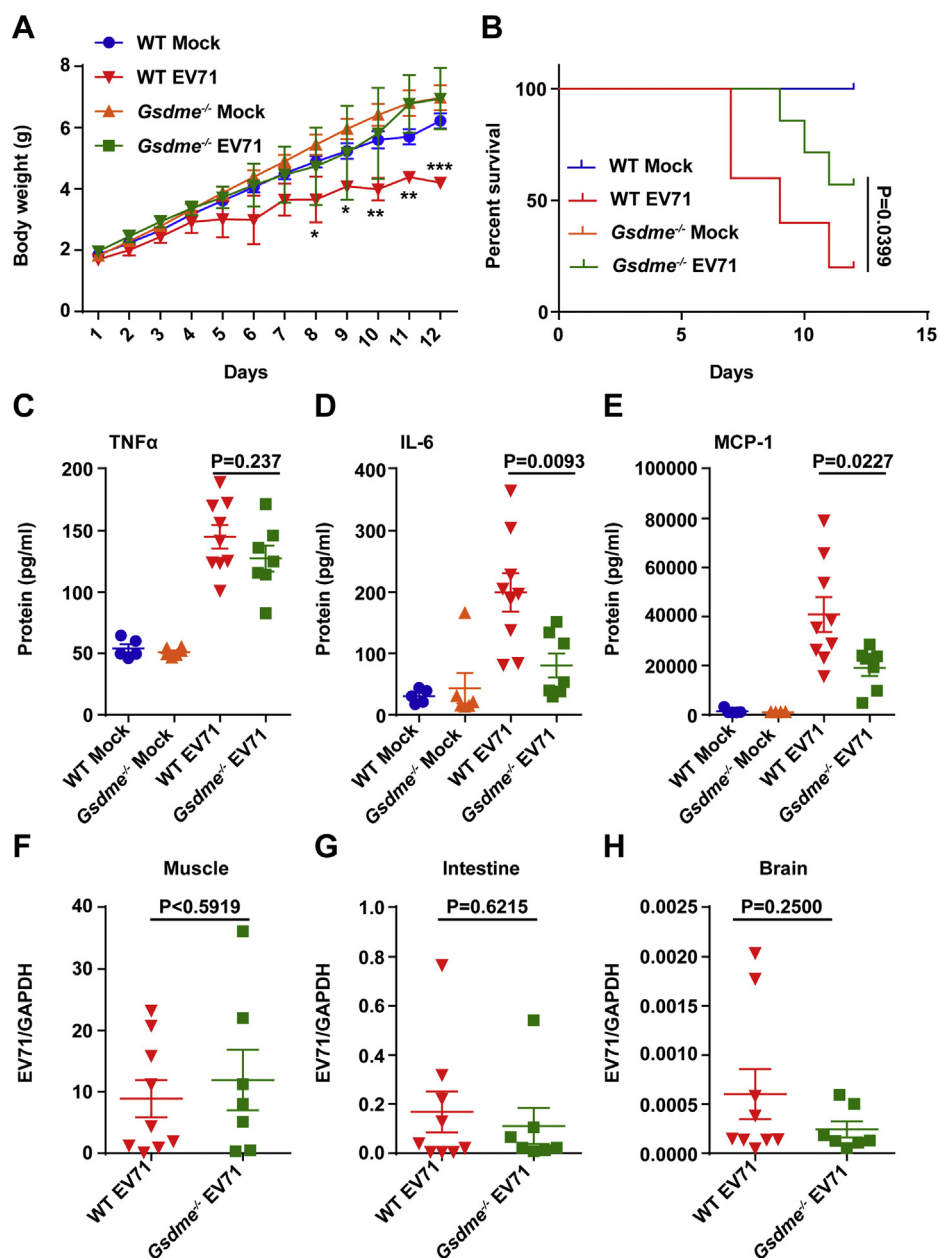
Figure 7. Survival rates in *Gsdme*⁻/⁻ mice infected with EV71. *A* and *B*, 3-day-old C57BL/6 WT and *Gsdme*⁻/⁻ mice were injected *via* the intraperitoneal route. The same volumes of DMEM were used as the control. Body weight (*A*) and survival rate (*B*) were monitored. All data are mean values ± SD. *$p < 0.05$, **$p < 0.01$. *C–E*, 3-day-old WT and *Gsdme*⁻/⁻ mice were infected with EV71 by intraperitoneal injection. At 3 DPI, peripheral blood samples were harvested and cytokine concentrations in the blood were analyzed by BDTM Cytometric Bead Array (CBA) Mouse Inflammatory Cytokines Kit (BD Biosciences). *p* Values are indicated. *F–H*, EV71 RNA levels in muscles, intestines, and brains were monitored in WT and *Gsdme*⁻/⁻ mice. One dot point indicates one animal. DMEM, Dulbecco's modified Eagle's medium; DPI, days postinfection; EV71, enterovirus 71; *Gsdme*, gasdermin E.

Q193-G194 pair and produces a truncated N-terminal fragment, GSDMD$_{1-193}$, which does not induce pyroptosis (40). However, cleavage of GSDME during EV71 infection is not induced by EV71 2A or 3C proteases (Fig. 3). EV71-induced caspase-3 activation is important for GSDME cleavage (Figs. 4 and 5). This is consistent with chemotherapeutic drug–induced GSDME cleavage at the D270-A271 pair (24, 25). How caspase-3 is activated by EV71 has been reported previously (41–45). EV71-induced caspase-3 activation may occur *via* two mechanisms: (1) EV71 infection induces cell death as intrinsic apoptosis or death receptor–dependent apoptosis

(41–43) and (2) EV71 infection induces conformational activation of proapoptotic protein Bax that translocates to the mitochondrial membrane and induces activation of caspase by releasing cytochrome *c* from mitochondria (44, 45). Recently, it has been reported that MCL-1 loss and BCL-xL inactivation following translation shutdown induced by viral infection were responsible for herpes simplex virus-1–induced caspase-3 activation and pyroptosis (46). Whether MCL-1 inhibition is involved in EV71-induced caspase-3 activation needs further investigation. A lack of GSDME or caspase-3 reduced the LDH release induced by EV71, especially in double-KO cells. In

GSDME-KO cells, EV71 infection partially induced LDH release. Although infrequent, morphological observation showed pyroptosis, which may be due to other GSDM family proteins cleaved by caspases in these cells. Which GSDM family protein or whether caspase-3 was involved in EV71-induced cell death in GSDME-KO cells requires further study.

Last, we verified the effect of GSDME on the pathogenesis of EV71 *in vivo*. There was no significant difference in weight loss between *Gsdme*^{−/−} and WT mice (Fig. 7A). Moreover, cytokines in the sera of *Gsdme*^{−/−} mice were similar to those in WT mice (Fig. 7, C–E). This is consistent with a previous report in which the development of *Gsdme*^{−/−} mice was normal (24). After EV7 infection, more *Gsdme*^{−/−} mice had survived compared with WT mice. This suggests that a lack of GSDME protects mice from the pathogenesis of EV71 infection. Considering a comparable viral load in both *Gsdme*^{−/−} and WT mice, it is tempting to speculate that reduced pyroptosis *in vivo* may be protective against EV71 infection. Alternatively, reduced tissue inflammation may alleviate EV71-mediated pathology. Further study is needed to clarify the underlying molecular mechanism. Collectively, our results support the conclusion that EV71 induces cleavage of GSDME in a caspase-3-dependent manner, and GSDME is necessary for the pathogenesis of EV71 infection *in vivo*.

In summary, EV71 infection induces cleavage of GSDME, which is activated specifically by caspase-3 activation. The D270-E271 pair of GSDME is crucial amino acid for caspase-3 cleavage. The D270E mutant of GSDME cannot be cleaved upon EV71 infection. Moreover, EV71 infection does not induce cleavage of GSDME in caspase-3-KO cells. *In vivo*, the GSDME-deficient mice showed a delay in the development of neurological symptoms and survived longer than WT mice during EV71 infection, which suggested that caspase-3 activation–mediated GSDME cleavage plays a critical role in the pathogenesis of EV71 infection.

Experimental procedures
Cell lines and viruses

HeLa, human neuroblastoma (SK-N-SH), human RD cells, and human embryonic kidney 293T cells were cultured in Dulbecco's modified Eagle's medium (Gibco) supplemented with 10% heat-inactivated fetal calf serum (Hyclone) and penicillin/streptomycin at 37 °C in a 5% CO_2 humidified atmosphere. EV71 infection was carried out as described previously (39–41).

Plasmids and antibodies

The GSDME (RC210515) and caspase-3 (RC223662) full-length plasmid was purchased from OriGene. The point mutation (D270A) was generated by PCR using KOD DNA polymerase (Toyobo). The plasmid that expresses EV71 3C or 2A was obtained as before description. The plasmids that express caspase-3 were purchased. All plasmids were verified by sequencing. Primary antibodies used were anti-DFNA5/

GSDME (abcam; catalog no.: ab215191), anti-EV71 (Millipore; catalog no.: MAB979), anti-β-actin (Sigma-Aldrich; catalog no.: A5441), anti-FLAG (Sigma-Aldrich; catalog no.: F3165), anti-Myc (Sigma-Aldrich; catalog no.: C3956), anti–eukaryotic translation initiation factor 4G (Santa Cruz; catalog no.: sc-373892), anti-V5 (Sigma-Aldrich; catalog no.: V8012), and anti-caspase-3 (Proteintech; catalog no.: 19677-1-AP; Cell Signaling Technology; catalog no.: 9662S).

Cell cytotoxicity and viability assay

The cell death and cell viability were analyzed by using the kit of CytoTox 96 Non-Radioactive Cytotoxicity Assay (G1780) and CellTiter-Glo luminescent cell viability assay (G7571) according to the manufacturer's instructions.

LDH is an indicator of cell membrane permeability. LDH release was detected by use of the CytoTox 96 Non-Radioactive Cytotoxicity Assay kit. HeLa cells were seeded in 96-well plate. Following EV71 infection, medium from the cells was transferred to a new 96-well plate, incubated with LDH working reagent for 30 min, and results were obtained at 490 nm by a spectrophotometer (40). The cells and supernatants were collected to analyze cell viability by using a CellTiter-Glo luminescent cell viability assay according to the manufacturer's instructions.

Immunofluorescence

Immunofluorescent assay was done as described previously (42). Briefly, cells were washed with PBS buffer and fixed with 4% formalin. Then cells were permeabilized with 0.5% Triton X-100. After cells were washed with PBS, they were blocked and stained with primary antibodies, followed by staining with an Alexa Fluor 488 secondary antibody. Nuclei were stained with 4',6-diamidino-2-phenylindole (Sigma). The cells were imaged on an Operetta instrument (PerkinElmer).

WB analysis

WB was used to analyze protein expression. In brief, protein samples from cultured cells were prepared by direct lysis in radioimmunoprecipitation assay buffer as described previously (47). After 30 min, cell lysates were centrifuged at 12,000 rpm for 10 min at 4 °C, and supernatants were used for SDS-PAGE and transferred to a nitrocellulose membrane. Membranes were blocked in 5% nonfat dried milk in PBS with Tween-20 at room temperature for 2 h and incubated with primary antibody (1:1000 dilution) overnight at 4 °C, followed with the corresponding IRDye Fluor 800–labeled immunoglobulin G or IRDye Fluor 680–labeled immunoglobulin G secondary antibody (LI-COR, Inc). Protein bands were visualized by using an Odyssey infrared imaging system at a wavelength of 700 to 800 nm and analyzed with Odyssey software Image Studio (LI-COR).

Quantitative real-time PCR analysis

Total RNA was extracted using TRLzol reagent (Invitrogen) from cell or tissue samples and reverse transcribed with M-MLV reverse transcriptase (Promega; catalog no.: M1750).

Real-time quantitative PCR was performed in 96-well plates; the reaction system included 2 µl diluted complementary DNA, 10 µM upstream primer, 10 µM downstream primer, 10 µl GOTaq green master mix, and nuclease-free water to 20 µl volume. The expression level of target gene was relative to that of GAPDH.

Construction of KO cell lines and ectopic expression of caspase-3 in the caspase-3 KO cells

The target sequence used is GGAAGCGAATCAATG-GACTC for human caspase-3. The target sequences used are TGAGTACATCGCCAAGGGTG or AATGGACTCTGGAA TATCCC for human GSDME. The KO cell lines were constructed as described previously (48). For reconstitution of caspase-3, caspase-3-deficient HeLa cells were seeded in 12-well plate 1 day before transfection at a concentration of 1.6×10^5 cells/well. Cells were transfected with 250 ng/well plasmid, which expresses caspase-3 for 24 h using Lipofectamine 2000 (Invitrogen).

EV71 infection in mice

The animal experiments were performed according to the protocols reviewed and approved by the Institute of Animal Use and Care Committee of the Institute of Laboratory Animal Science, Peking Union Medical College (BYS19002).

$Gsdme^{-/-}$ mice were provided by Professor Feng Shao (National Institute of Biological Sciences) (24). WT C57BL/6 mice were purchased from Vital River Laboratory Animal Technology Co and maintained at the Specific Pathogen Free (SPF) Laboratory Animal facility. All animal care and experimental procedures were complied with national guidelines and approved by the Animal Ethics and Experimentation Committee of the Institute of Pathogen Biology of the Chinese Academy of Medical Sciences.

Three-day-old sulking mice (1.69–2.14 g) were challenged with 10^6 pfu EV71 (strain 695F) by intraperitoneal route (27). Additional C57BL/6 or $Gsdme^{-/-}$ mice were injected with Dulbecco's modified Eagle's medium as control. The weight, symptoms, and survival rates of the infected mice were monitored daily for 12 days.

Statistics

The two-tailed Student's t test was used for two-group comparisons. The $p < 0.05$ (*), $p < 0.01$(**), and $p < 0.001$(***) values were considered significant. NS stands for not significant.

Data availability

All data are contained within the article.

References

1. Schmidt, N. J., Lennette, E. H., and Ho, H. H. (1973) An apparently new enterovirus isolated from patients with disease of the central nervous system. *J. Infect. Dis.* **129**, 304–309
2. Solomon, T., Lewthwaite, P., Perera, D., Cardosa, M. J., McMinn, P., and Ooi, M. H. (2010) Virology, epidemiology, pathogenesis, and control of enterovirus 71. *Lancet Infect. Dis.* **10**, 778–790
3. Chan, L. G., Parashar, U. D., Lye, M. S., Ong, F. G., Zaki, S. R., Alexander, J. P., Ho, K. K., Han, L. L., Pallansch, M. A., Suleiman, A. B., Jegathesan, M., and Anderson, L. J. (2000) Deaths of children during an outbreak of hand, foot, and mouth disease in sarawak, Malaysia: Clinical and pathological characteristics of the disease. For the outbreak study group. *Clin. Infect. Dis.* **31**, 678–683
4. Huang, C. C., Liu, C. C., Chang, Y. C., Chen, C. Y., Wang, S. T., and Yeh, T. F. (1999) Neurologic complications in children with enterovirus 71 infection. *N. Engl. J. Med.* **341**, 936–942
5. Ho, M., Chen, E. R., Hsu, K. H., Twu, S. J., Chen, K. T., Tsai, S. F., Wang, J. R., and Shih, S. R. (1999) An epidemic of enterovirus 71 infection in Taiwan. Taiwan enterovirus epidemic working group. *N. Engl. J. Med.* **341**, 929–935
6. Xing, W., Liao, Q., Viboud, C., Zhang, J., Sun, J., Wu, J. T., Chang, Z., Liu, F., Fang, V. J., Zheng, Y., Cowling, B. J., Varma, J. K., Farrar, J. J., Leung, G. M., and Yu, H. (2014) Hand, foot, and mouth disease in China, 2008-12: An epidemiological study. *Lancet Infect. Dis.* **14**, 308–318
7. Ooi, M. H., Wong, S. C., Lewthwaite, P., Cardosa, M. J., and Solomon, T. (2010) Clinecal features, diagnosis, and management of enterovirus 71. *Lancet Neurol.* **9**, 1097–1105
8. McMinn, P., Stratov, I., Nagarajan, L., and Davis, S. (2001) Neurological manifestations of enterovirus 71 infection in children during an outbreak of hand, foot, and mouth disease in Western Australia. *Clin. Infect. Dis.* **32**, 236–242
9. McMinn, P. C. (2002) An overview of the evolution of enterovirus 71 and its clinical and public health significance. *FEMS Microbiol. Rev.* **26**, 91–107
10. Chang, L., Lin, T., Hsu, K., Huang, Y., Lin, K., Hsueh, C., Shih, S., Ning, H., Hwang, M., Wang, H., and Lee, C. (1999) Clinical features and risk factors of pulmonary oedema after enterovirus-71-related hand, foot, and mouth disease. *Lancet* **354**, 1682–1686

11. Chen, Y., Yu, C., Wang, Y., Liu, C., Su, I., and Lei, H. (2004) A murine oral enterovirus 71 infection model with central nervous system involvement. *J. Gen. Virol.* **1**, 69–77

12. Wang, Y., Chou, C., Lei, H., Liu, C., Wang, S., Yan, J., Su, I., Wang, J., Yeh, T., Chen, S., and Yu, C. K. (2004) A mouse-adapted enterovirus 71 strain causes neurological disease in mice after oral infection. *J. Virol.* **15**, 7916–7924

13. Liu, M., Lee, Y., Wang, Y., Lei, H., Liu, C., Wang, S., Su, I., Wang, J., Yeh, T., Chen, S., and Yu, C. (2005) Type I interferons protect mice against enterovirus 71 infection. *J. Gen. Virol.* **12**, 3263–3269

14. Miao, E. A., Leaf, I. A., Treuting, P. M., Mao, D. P., Dors, M., Sarkar, A., Warren, S. E., Wewers, M. D., and Aderem, A. (2010) Caspase-1-induced pyroptosis is an innate immune effector mechanism against intracellular bacteria. *Nat. Immunol.* **11**, 1136–1142

15. Lamkanfi, M., and Dixit, V. M. (2014) Mechanisms and functions of inflammasomes. *Cell* **5**, 1013–1022

16. Ding, J., Wang, K., Liu, W., She, Y., Sun, Q., Shi, J., Sun, H., Wang, D. C., and Shao, F. (2016) Pore-forming activity and structural autoinhibition of the gasdermin family. *Nature* **7610**, 111–116

17. Shi, J., Zhao, Y., Wang, K., Shi, X., Wang, Y., Huang, H., Zhuang, Y., Cai, T., Wang, F., and Shao, F. (2015) Cleavage of GSDMD by inflammatory caspases determines pyroptotic cell death. *Nature* **7575**, 660–665

18. Kayagaki, N., Stowe, I. B., Lee, B. L., O'Rourke, K., Anderson, K., Warming, S., Cuellar, T., Haley, B., Roose-Girma, M., Phung, Q. T., Liu, P. S., Lill, J. R., Li, H., Wu, J., Kummerfeld, S., *et al.* (2015) Caspase-11 cleaves gasdermin D for non-canonical inflammasome signalling. *Nature* **7575**, 666–671

19. Chen, X., He, W. T., Hu, L., Li, J., Fang, Y., Wang, X., Xu, X., Wang, Z., Huang, K., and Han, J. (2016) Pyroptosis is driven by non-selective gasdermin-D pore and its morphology is different from MLKL channel-mediated necroptosis. *Cell Res* **9**, 1007–1020

20. Liu, X., Zhang, Z., Ruan, J., Pan, Y., Magupalli, V. G., Wu, H., and Lieberman, J. (2016) Inflammasome-activated gasdermin D causes pyroptosis by forming membrane pores. *Nature* **535**, 153–158

21. He, W. T., Wan, H., Hu, L., Chen, P., Wang, X., Huang, Z., Yang, Z. H., Zhong, C. Q., and Han, J. (2015) Gasdermin D is an executor of pyroptosis and required for interleukin-1beta secretion. *Cell Res.* **25**, 1285–1298

22. Shi, J., Gao, W., and Shao, F. (2017) Pyroptosis: Gasdermin-mediated programmed necrotic cell death. *Trends Biochem. Sci.* **4**, 245–254

23. Sborgi, L., Ruhl, S., Mulvihill, E., Pipercevic, J., Heilig, R., Stahlberg, H., Farady, C. J., Muller, D. J., Broz, P., and Hiller, S. (2016) GSDMD membrane pore formation constitutes the mechanism of pyroptotic cell death. *EMBO J.* **35**, 1766–1778

24. Wang, Y., Gao, W., Shi, X., Ding, J., Liu, W., He, H., Wang, K., and Shao, F. (2017) Chemotherapy drugs induce pyroptosis through caspase-3 cleavage of a gasdermin. *Nature* **7661**, 99–103

25. Rogers, C., Fernanders-Alnemri, T., Mayes, L., Alnemri, D., Cingolani, G., and Alnemri, E. S. (2017) Cleavage of DFNA5 by caspase-3 during apoptosis mediates progression to secondary necrotic/pyroptotic cell death. *Nat. Commun.* **8**, 14128

26. Rogers, C., Erkes, D. A., Nardone, A., Aplin, A. E., Fernandes-Alnemri, T., and Alnemri, E. S. (2019) Gasdermin pores permeabilize mitochondria to augment caspase-3 activation during apoptosis and inflammasome activation. *Nat. Commun.* **1**, 1689

27. Zhang, X., Song, Z., Qin, B., Zhang, X., Chen, L., Hu, Y., and Yuan, Z. (2013) Rupintrivir is a promising candidate for treating severe cases of enterovirus-71 infection: Evaluation of antiviral efficacy in a murine infection model. *Antivir. Res.* **3**, 264–269

28. Fink, S. L., and Cookson, B. T. (2007) Pyroptosis and host cell death responses during Salmonella infection. *Cell Microbiol* **9**, 2562–2570

29. Li, M. L., Hsu, T. A., Chen, T. C., Chang, S. C., Lee, J. C., Chen, C. C., Stollar, V., and Shih, S. R. (2002) The 3C protease activity of enterovirus 71 induces human neural cell apoptosis. *Virology* **293**, 386–395

30. Li, M. L., Lin, J. Y., Chen, B. S., Weng, K. F., Shih, S. R., Calderon, J. D., Tolbert, B. S., and Brewer, G. (2019) EV71 3C protease induces apoptosis by cleavage of hnRNP A1 to promote apaf-1 translation. *PLoS One* **9**, e022048

31. Kuo, R. L., Kung, S. H., Hsu, Y. Y., and Liu, W. T. (2002) Infection with enterovirus 71 or expression of its 2A protease induces apoptotic cell death. *J. Gen. Virol.* **83**, 1367–1376

32. Li, H., Bai, Z., Li, C., Sheng, C., and Zhao, X. (2020) EV71 infection induces cell apoptosis through ROS generation and SIRT1 activation. *J. Cell. Biochem.* **121**, 4321–4331

33. Wang, H., Lei, X., Xiao, X., Yang, C., Lu, W., Huang, Z., Leng, Q., Jin, Q., He, B., Meng, G., and Wang, J. (2015) Reciprocal Regulation between enterovirus 71 and the NLRP3 inflammasome. *Cell. Rep.* **12**, 42–48

34. Kayagaki, N., Warming, S., Lamkanfi, M., Vande Walle, L., Louie, S., Dong, J., Newton, K., Qu, Y., Liu, J., Heldens, S., Zhang, J., Lee, W. P., Roose-Girma, M., and Dixit, V. M. (2011) Non-canonical inflammasome activation targets caspase-11. *Nature* **479**, 117–121

35. Shi, J., Zhao, Y., Wang, Y., Gao, W., Ding, J., Li, P., Hu, L., and Shao, F. (2014) Inflammatory caspases are innate immune receptors for intracellular LPS. *Nature* **514**, 187–192

36. Jorgensen, I., Rayamajhi, M., and Miao, E. A. (2017) Programmed cell death as a defence against infection. *Nat. Rev. Immunol.* **3**, 151–164

37. Aglietti, R. A., Estevez, A., Gupta, A., Ramirez, M. G., Liu, P. S., Kayagaki, N., Ciferri, C., Dixit, V. M., and Dueber, E. C. (2016) GsdmD p30 elicited by caspase-11 during pyroptosis forms pores in membranes. *Proc. Natl. Acad. Sci. U. S. A.* **113**, 7858–7863

38. Bai, J., Chen, X., Liu, Q., Zhou, X., and Long, J. (2019) Characteristics of enterovirus 71-induced cell death and genome scanning to identify viral genes involved in virus-induced cell apoptosis. *Virus Res.* **265**, 104–114

39. Wang, W., Xiao, F., Wan, P., Pan, P., Zhang, Y., Liu, F., Wu, K., Liu, Y., and Wu, J. (2017) EV71 3D protein binds with NLRP3 and enhances the assembly of inflammasome complex. *PLoS Pathog.* **1**, e1006123

40. Lei, X., Zhang, Z., Xiao, X., Qi, J., He, B., and Wang, J. (2017) Enterovirus 71 inhibits pyroptosis through cleavage of Gasdermin D. *J. Virol.* **91**, e01069-17

41. Wang, C., Zhou, R., Zhang, Z., Jin, Y., Cardona, C. J., and Xing, Z. (2015) Intrinsic apoptosis and proinflammatory cytokines regulated in human astrocytes infected with enterovirus 71. *J. Gen. Virol.* **96**, 3010–3022

42. Shi, W., Li, X., Hou, X., Peng, H., Jiang, Q., Shi, M., Ji, Y., Liu, X., and Liu, J. (2012) Differential apoptosis gene expressions of rhabdomyosarcoma cells in response to enterovirus 71 infection. *BMC Infect. Dis.* **12**, 327

43. Chen, L. C., Shyu, H. W., Chen, S. H., Lei, H. Y., Yu, C. K., and Yeh, T. M. (2006) Enterovirus 71 infection induces Fas ligand expression and apoptosis of Jurkat cells. *J. Med. Virol.* **78**, 780–786

44. Cong, H., Du, N., Yang, Y., Song, L., Zhang, W., and Tien, P. (2016) Enterovirus 71 2B induces cell apoptosis by directly inducing the conformational activation of the proapoptotic protein Bax. *J. Virol.* **90**, 9862–9877

45. Han, X., and Cong, H. (2017) Enterovirus 71 induces apoptosis by directly modulating the conformational activation of pro-apoptotic protein Bax. *J. Gen. Virol.* **98**, 422–434

46. Orzalli, M. H., Prochera, A., Payne, L., Smith, A., Garlick, J. A., and Kagan, J. C. (2021) Virus-mediated inactivation of anti-apoptotic Bcl-2 family members promotes Gasdermin-E-dependent pyroptosis in barrier epithelial cells. *Immunity* **54**, 1447–1462

47. Lei, X., Liu, X., Ma, Y., Sun, Z., Yang, Y., Jin, Q., He, B., and Wang, J. (2010) The 3C protein of enterovirus 71 inhibits retinoid acid-inducible gene I-mediated interferon regulatory factor 3 activation and type I interferon responses. *J. Virol.* **84**, 8051–8061

48. Lei, X., Xiao, X., Zhang, Z., Ma, Y., Qi, J., Wu, C., Xiao, Y., Zhou, Z., He, B., and Wang, J. (2017) The Golgi protein ACBD3 facilitates Enterovirus 71 replication by interacting with 3A. *Sci. Rep.* **7**, 44592